Proc. Natl. Acad. Sci., India, Sect. A Phys. Sci. (October–December 2017) 87(4):567–579
https://doi.org/10.1007/s40010-017-0435-9

REVIEW ARTICLE

Airborne LiDAR Technology: A Review of Data Collection and Processing Systems

Bharat Lohani[1] · **Suddhasheel Ghosh**[2]

Received: 3 July 2017 / Revised: 15 August 2017 / Accepted: 15 September 2017 / Published online: 17 November 2017

Abstract Airborne light detection and ranging (LiDAR) has now become industry standard tool for collecting accurate and dense topographic data at very high speed. These data have found use in many applications and several new applications are being discovered regularly. This paper presents a review of the current state-of-the-art of this technology. The paper covers both data capture and data processing issues of the technology. The paper first discusses various types of LiDAR sensors and their working. This is followed by information on data format and data quality assessment procedures. The paper reviews the existing data classification techniques and also looks into the new approaches like convolutional neural networks and visual analytics for data processing. Finally, the paper outlines future scope of the technology and the research challenges, which should be addressed in coming years.

Keywords LiDAR · Procurement · Processing · Classification · Visualization

1 Introduction

Shortly after the development of the first optical laser, instruments employing this new technology were developed to measure distance by timing round trip travel of a laser pulse between the laser transmitter, the surface being measured and the laser receiver [1]. The concept of using airborne laser to measure terrestrial biomass emerged during the 1960s and 1970s. Rempel and Parker [2] proposed the idea of using an airborne laser for micro-relief studies in 1964. For the first time, Hickman and Hogg [3] demonstrated the use of the laser for bathymetry measurements in 1968. Hoge et al. [4] reported the results of a study using the NASA (National Aeronautics and Space Administration) airborne oceanographic LiDAR (AOL) to derive water depths in the Atlantic Ocean and more turbid Chesapeake Bay. A major hindrance in the earlier uses, as noted by Krabill et al. [5] and Schreier et al. [6], was locating the position of the airborne laser; Hoge et al. [7] mentioned the use of tracking radar, Arp et al. [8] used the Autotape to measure the position of a floating helicopter by resection, and Schreier et al. [6] described a photogrammetric method. Accurate positioning of airborne lasers only became possible with the advent of Global Positioning System (GPS). Further advancement in Inertial Measuring Unit (IMU), laser, and computing technologies made the use of LiDAR cheaper and more accurate. In the last two decades, the airborne remote sensing sector has seen this technology emerge as an extremely rapid and highly accurate terrain-mapping tool. This development has resulted in innovative solutions to difficult mapping problems, including several new applications which were nearly impossible earlier in the absence of data like LiDAR.

The main aim of this paper is to review the status of LiDAR technology, highlight the research issues associated with the technology and identify the direction where the technology is heading to. The review will be carried out for different aspects viz., data collection, data processing, accuracy analysis, data classification, data visualization and finally applications being realized and the future potential of the technology. LiDAR technology can be

✉ Bharat Lohani
blohani@iitk.ac.in

[1] Department of Civil Engineering, Indian Institute of Technology Kanpur, Kanpur, India

[2] Department of Civil Engineering, MGM's Jawaharlal Nehru Engineering College, Aurangabad, India

operated using different platforms, viz., space vehicles, aircrafts and helicopters, drones, ground based vehicles, and tripods. While the basic principle of the technology in each case is same, there are some differences in data capture procedures, data processing steps, applications of data etc. The current paper is specifically focused on airborne LiDAR technology.

2 Principle of LiDAR Technology

As shown in Fig. 1, an airborne LiDAR system consists of (1) an airborne platform (aircraft or helicopter), which is used to fly a LiDAR sensor over an area of interest; (2) LiDAR sensor, which is used to generate short width laser pulses (of the order of a few nano-seconds), transmit these toward ground, scan the ground beneath while firing pulses, receive the return signal (i.e., return waveform), measure the time of travel of the return pulse (most significant return, first return, last return, or multiple returns), associate each return pulse with Global Navigation Satellite System (GNSS) time and the scan angle at which the pulse was transmitted; (3) a GNSS receiver, which works in tandem with a ground based GNSS base station receiver and observes the position of the aircraft at each epoch of GNSS observation (1 or 2 Hz); (4) an IMU sensor, which observes the accelerations and orientations of the aircraft at a much higher frequency than that of GNSS epoch (say 400 Hz); (5) an onboard computer, which timestamps different data produced by the above sensors using the GNSS time and archives raw data. It is a common practice to also fly a medium format digital camera (60–100 MP) along with LiDAR sensor as it provides color information of the terrain.

The processing steps for data collected using various sensorsare shown in Fig. 2. Accurate position [< 2 cm circular error probable (CEP)] of the aircraft is determined by differential processing of the onboard and reference GNSS receivers (which collect multi-constellation, multi-frequency, carrier phase GNSS signals). The trajectory (i.e. the location and orientation of the aircraft at the time of firing of each laser pulse) is then computed by integrating GNSS solution with the IMU observations. Through the geolocation process (as shown in Hofton et al. [9]) the laser ranges and scanning angles are attached with the aircraft trajectory to yield the coordinates of the point on the ground in GNSS coordinate system, i.e., ECEF WGS-84 (Earth Centered Earth Fixed World Geodetic System) Cartesian coordinate system. The system calibration parameters are also input to the processing software at this stage to minimize certain errors. The coordinates generated can then be transformed to any desired horizontal and vertical datum.

3 Different Forms of LiDAR Sensors

A major part of the last two decades has been dominated by single wavelength single pulse Linear Mode LiDAR (LML) with single or multi-pulse ability. However, recently several new forms of LiDAR sensors have also

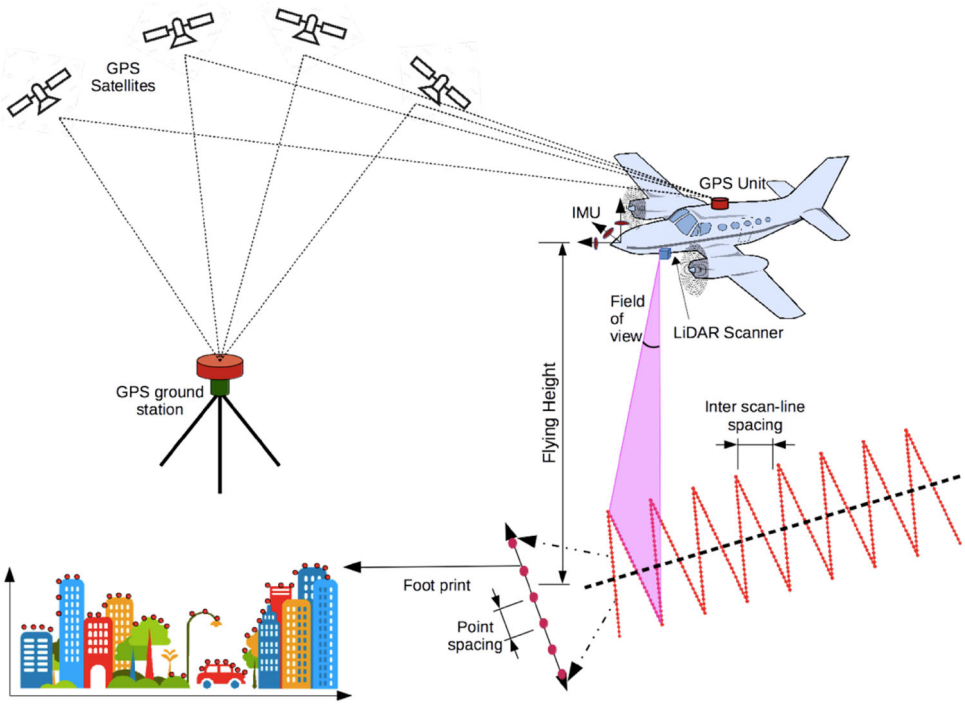

Fig. 1 Airborne LiDAR data capture. Red dots show LiDAR data on terrain objects

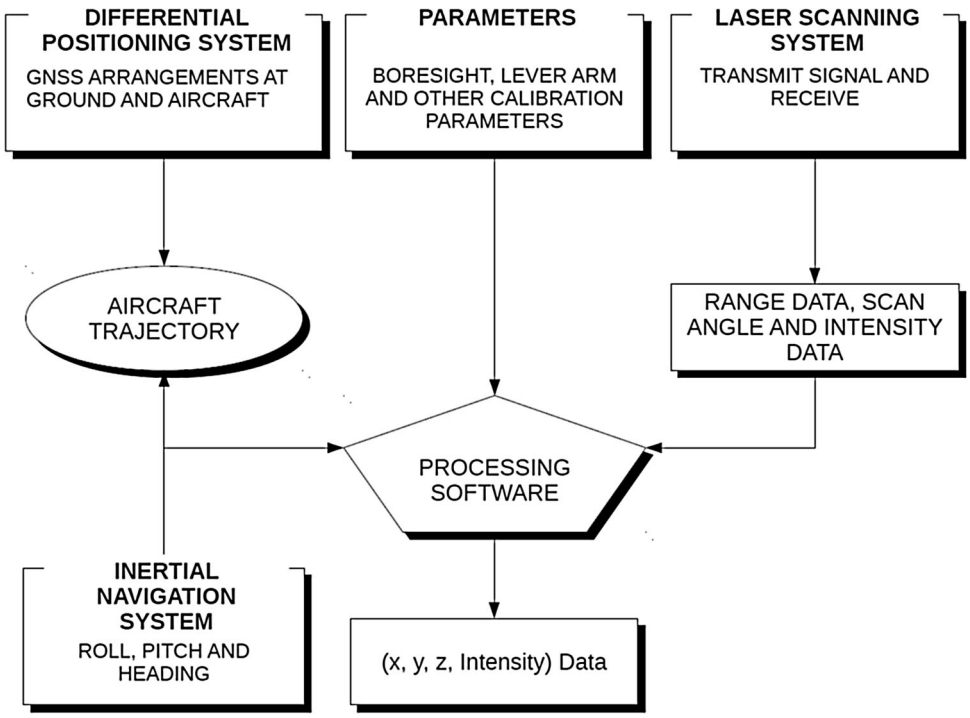

Fig. 2 Schematic display of processing flow of LiDAR system

appeared and are opening new applications. This section will briefly discuss these different forms of LiDAR sensors.

3.1 Single Pulse Single Wavelength Linear Mode LiDAR (LML)

In these LiDAR sensors, a single laser pulse is transmitted and received at the sensor. Any two consecutive pulses are separated by enough time gap so the next pulse is transmitted only after the previous pulse has been received. Pulse Repetition Frequency (PRF) of the order of 400 kHz is possible with the help of current scanners available in market. In general, infra-red wavelengths are employed as their reflection from most of the topographic features is significant enough to register its return on receiver thus producing a coordinate. The most common scanning mechanism employed in these sensors is zig-zag or parallel line patterns. A few sensors have also been proposed with elliptical scanning. LML sensors have limitation in terms of flying altitude as higher altitude leads to reduction in the PRF and also the energy of the signal reaching the receiver diminishes. These sensors are good for small area survey, say up to 2000–3000 sq km, when compared to new Geiger Mode LiDAR/Single Photon LiDAR (GML/SPL) sensors, though the former have been successfully employed for surveying areas of several tens of thousands of square kilometers. The advantage of LML is that they also generate intensity image unlike GML and can generate data also for power lines unlike GML/SPL.

3.2 Multi-pulse in Air (MPiA) LiDAR

In case of single pulse LiDAR the pulses are transmitted sequentially, as there is no method to distinguish between these pulses. This limits the PRF and flying altitude. Multiple Pulses in Air Technology, or MPiA, allows airborne LIDAR system to fire the second laser pulse prior to the receipt of the previous pulse's return waveform, leading to doubling of the pulse rate at any given altitude. This permits higher pulse rates than previously possible by single pulse LiDAR. Besides this major change the functioning of this sensor is similar to the LML. The role of Multi-pulse would reduce in future as higher data density from higher heights are now being generated by GML/SPL. However, there is difference in data characteristics between MPiA and GML/SPL, as MPiA data are similar to LML with certain advantages.

3.3 Full Waveform Digitization (FWD) LiDAR

In case of full waveform digitization, the return waveform is completely digitized at fine time intervals, e.g. 1 ns. This, therefore, unlike single or multiple returns, captures the property of the backscattering surfaces in the entire depth of a footprint. It is then possible to determine the significant backscattering surfaces within the footprint by using techniques like Gaussian Decomposition [10]. FWD data have been found more suitable for identification of objects under canopy and detecting the ground [11]. The

use of FWD is very much application dependent. Several LML sensors also support FWD now.

3.4 Multi-spectral LiDAR (MSL)

The intensity of the return pulse can help in the classification of LiDAR data, similar to the case of images. Due to this reason, the same has been widely investigated by various researchers including the work on normalization of return intensity for different ranges and angles. However, with only a single wavelength (with narrow bandwidth) the accuracy of classification is limited. In case of the multi-spectral LiDAR (e.g. TITAN, by Teledyne Optech Inc.), three independent pulses—wavelengths 532, 1064 and 1550 nm—are emitted, each with a 300 kHz PRF. The multi-spectral LiDAR has potential to be used for 3D land cover classification as shown by Xiaoliang et al. [12] and environmental applications. While MSL offers multi-wavelength view and increased data density, the same can be achieved also by flying a multi-spectral or hyper-spectral sensor with LML. If the demand of the application is spectral analysis along with geometric information, the latter options are more suitable.

3.5 Geiger Mode LiDAR (GML) and Single Photon LiDAR (SPL)

The technologies of GML and SPL share their principle, though these are being promoted by two different companies, viz., Harris Corporations and SigmaSpace (Hexagon group company), respectively. Unlike Linear Mode LiDAR, both GML and SPL can measure range by detecting even a single photon of return laser. In these sensors, similar to LML, the sensor is fitted at the bottom of an aircraft looking downward. The scanner scans in a circular pattern while the aircraft moves ahead. A laser pulse is split into multiple pulselets (100 in case of the SPL from SigmaSpace). Around 60,000 such sets of pulselets are generated every second, thereby producing 6 Million possible measurements every second. The typical circular scan pattern ensures full coverage around high rise buildings thus minimizing the presence of shadows in data. The main advantage of these sensors is to generate highly dense point cloud from flying heights of order of 2000–10,000 m, which is not possible in case of LML. However, unlike LML, these sensors do not produce multiple returns or full waveforms and have also been found to produce less accurate data for highly reflective surfaces [13]. Moreover, these sensors are especially suitable for large area survey where only digital elevation model is required, e.g., 3DEP program of USA. In general, these sensors become cost-effective for areas beyond 2000 sq km.

4 Flight Planning for Airborne LiDAR and Photograph

While performing flying operations for LiDAR data acquisition, aircraft covers the area of interest (AOI) on terrain in parallel strips. After flying over a strip, aircraft turns to the next strip. In order to acquire data with desired characteristics (namely data density, overlap, uniform distribution, spacing and accuracy) the operating parameters of LiDAR sensor and flying parameters of aircraft need to be decided in advance and accordingly the project is undertaken. However, there can be a large number of sets of sensor and flight parameters which can result in the desired data, but would take different flying hours. Minimization of flying hours is important to reduce the cost of a project. In view of this, flight planning is carried out prior to airborne LiDAR data acquisition in field. Flight planning generates the sensor and flight parameters which would guarantee the desired data characteristics and also minimize the cost of data acquisition [14]. In the case of total manual or semi-automatic solution of this problem [assisted by software like ASCOT (by Leica), ALTM-NAV (by Optech), and IGIplan (by IGI)] there is no guarantee of reaching the optimal solution. Furthermore, the solution can be highly biased by the experience of the persons involved. Therefore, it is requiredto research in developing optimization based solution for this problem.

One such work has addressed numerous research issues of flight planning for airborne LiDAR data acquisition in a series of publications [14–20]. The researchers conceptualized a comprehensive flight planning system that consists of various components of flight planning (e.g., data requirements, mapping requirements, sensor characteristics, aerial platforms, field limitations, flight duration, optimization algorithms, and simultaneous data acquisition with multiple sensors). The proposed flight planning system closely mimics flying operations and estimates the actual cost of data acquisition as the estimated flight duration consists of both turning time and strip time. Further, the system includes all data characteristics as constraints and uses evolutionary algorithms to determine an optimal solution. Furthermore, the flexible system design facilitates modification of any component and its inter-relation with other components and thus higher level of abstraction can be adopted at any stage. Consequently, the system shows a capacity to simulate the most realistic scenario of airborne data acquisition with minimum user intervention. The demonstrated system in this research provides flight plan, flight planning parameters, and turning mechanisms as an output. There is a need to further research this area and implement the solutions during field operations.

5 LiDAR Data and File Format

LiDAR data generated by different types of sensors primarilyconsist of the coordinates of points (i.e., X, Y, Z), intensity of return (I), associated color information (R, G, B) which is taken corresponding to each point from the simultaneously flown camera and GNSS time when the points are captured. Besides this the data also contains information about its return number, number of returns for a pulse, the scan angle, data-on-edge-of-scan information, land cover class associated with data point etc. All these information about data are stored in .las file format [21]. The .las format has evolved from its earlier version 1.0 to now 1.4 and has provision to store waveform data as well. One example of LiDAR data displayed with elevations as colors and intensity data as gray scale are shown in Fig. 3.

6 Accuracy Analysis of LiDAR Data

LiDAR data generated in field need to undergo quality check. An elaborate quality check methodology covering various aspects of LiDAR data is suggested in United States Geological Survey (USGS) Base Specifications document [22]. Though primary purpose of this document is to specify data for National Geospatial Program in USA, the procedures are applicable in nearly all projects. The vertical accuracy of LiDAR is of prime importance. Therefore, multiple measures for vertical accuracy are suggested. The basis for vertical accuracy is the Root Mean Square Error (RMSE), which is computed by comparing LiDAR points with the ground surveyed points. The vertical accuracies are reported as non-vegetated vertical accuracy (NVA) and vegetated vertical accuracy (VVA). Check points for NVA are surveyed in clear, open areas, devoid of vegetation and other vertical artifacts, where only single returns are possible. NVA is computed as $1.96 \times \mathrm{RMSE}_z$. For determining VVA, the checkpoints should be surveyed in vegetated areas where multiple returns are common. This is computed as the 95th percentile of the differences in LiDAR and reference data, as in these data do not follow normal distribution.

Unlike vertical accuracy, planimetric accuracy of LiDAR data always poses a problem of determination in field. There are a few indirect methods to determine this accuracy using reference objects, e.g., corners of building or specially installed targets. The planimetric accuracy is stated as $1.7308 \times \mathrm{RMSE}_r$, where $RMSE_r$ is the Root Mean Square Error in horizontal computed by comparing LiDAR data with ground reference. There have been attempts to determine planimetric accuracy using more direct approaches like Casella et al. [23] and Vosselman [24]. However, these methods under-estimate the planimetric accuracy. A method which can determine correct planimetric accuracy of LiDAR is not yet available.

In addition to the accuracy there are several other quality parameters against which data captured should be evaluated. Nominal Pulse Spacing (NPS) is a measure of nearness of data points and is defined as the average data spacing between data points. This is determined for first return data of middle 90% of a flight swath. Similar to NPS, Nominal Pulse Density (NPD) is defined as the number of data points per square meter. Aggregate NPS and NPD are reported when instead of single swath aggregate data from multiple swaths are available for same spatial location. NPS and data density have inverse relation. LiDAR data captured should not possess voids except for those areas wherefrom laser does not reflect, e.g., water bodies. The area of such voids, within a single swath for first return data, should not be larger than $(4 \times \mathrm{NPS})^2$. For any application, uniform spatial distribution of LiDAR data is crucial. Data density alone does not represent spatial distribution. Spatial distribution of LiDAR data is determined by counting the grid cells, which have at least one first return data inside them, where the size of grid cell laid over data is 2xNPS. As per the USGS base specification at least 90% grid cells should have at least one data point.

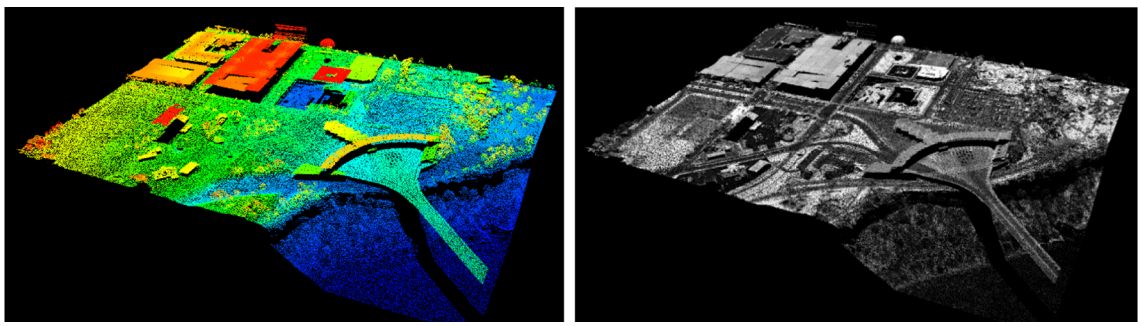

Fig. 3 Example of LiDAR data. Image on left shows point cloud colored as per height while image on right is the corresponding intensity image. Colours or gray level shades are to show relative heights or intensity levels, respectively, and therefore no legends are given (courtesy Optech Inc.)

7 Visualization of LiDAR Data

As a first step in LiDAR data analysis it is necessary to visualize point cloud using interactive approaches. Geovisualization is a wide area of research and contributes toward visualization of LiDAR data as well. There are a range of techniques for visualization of LiDAR data which are already available in the body of research literature. These techniques include (1) projection of 3D data to 2D raster and treat the data as an image for color scale visualization, (2) visualization of data in 2.5D using DSM(Digital Surface Model) and DEM(Digital Elevation Model) generated from LiDAR data, (3) generating 2D triangulation and 3D tetrahedralization using Delaunay Triangulation methods and visualize the data as 2.5D, (4) generate contours from LiDAR DEM and visualize the same, and (5) conversion of 3D LiDAR data into two stereo-pairs and visualization of the same using stereovision.

Kreylos et al. [25] and Richter and Döllner [26] have attempted the visualization of point cloud data using out-of-core computation methods. Point cloud data were converted to voxels and visualized by Stoker [27, 28], whereas Isenburg [29] generated raster Digital Elevation Model (DEM) via a Triangulated Irregular Network (TIN) streaming technique. In the context of various visualization schemes for LiDAR data, Ghosh and Lohani [30, 31] carried out extensive investigations and concluded that data visualization in stereoscopic mode has potential to provide more immersive visualization experience. They further developed a pipeline for visualization of LiDAR data in stereoscopic manner, which provides lighter data and avoids confusion of visualization of point cloud alone. In this pipeline first using Density Based Spatial Clustering of Application with Noise (DBSCAN) [32] and Ordering Points to Identify the Clustering Structure (OPTICS) [33], Ghosh and Lohani attempted to cluster LiDAR data [31]. They found DBSCAN to perform better than the OPTICS algorithm in terms of computational time, and performance of clustering. Subsequently, the clusters generated by DBSCAN were classified into three different types: (1) sparse and wide clusters, (2) dome shaped clusters, and (3) clusters potentially containing planes. The clusters were treated by a processing pipeline [25] to visualize them. The comparison of various existing processing pipelines reveals that the visualization pipeline developed by Ghosh and Lohani [30], performed almost equivalent to the Computer Aided Design (CAD) based pipeline [34].

8 Processing LiDAR Data for Scene Understanding

Unlike image data LiDAR data are geometric representation of terrain. Though LiDAR data are accompanied by intensity and sometime RGB information, the prime source of object recognition in LiDAR data is its geometry. Therefore, the approaches aimed at identification, extraction and classification of objects in LiDAR data are primarily based on exploiting the geometric properties, which sometime are also assisted by intensity and RGB data. Further, unlike image classification where all classes are classified simultaneously, the approaches, in general, for LiDAR data have focused on identification of one object at a time. The following paragraphs outline the state-of-the-art in this domain.

8.1 Ground Classification (Ground Filtering)

Literature suggests that most of the approaches begin with outlier detection and removal, which is followed by "ground filtering". The process of filtering involves the labelling of the dataset into terrain and non-terrain points. Various filtering algorithms have been reviewed by Sithole and Vosselman [35], Kobler et al. [36], Pfeifer and Mandlberger [37] and Meng et al. [38]. It is worthwhile to mention here that after a comparison of filtering algorithms, Sithole and Vosselman [39] had suggested, and Błaszczak-Bąket al. [40] have reiterated that there is no unique algorithm for extracting all types of terrains.

The literature on ground detection algorithms designed for LiDAR data can be classified in the following groups: (1) morphological filters and their variants, (2) active contouring, (3) progressive densification, (4) spline-based methods, (5) surface based filters and their extensions and variants, and (6) repetitive interpolation. The literature found in these areas are given in Table 1.

Despite a large body of literature on ground classification and commercial tools available, manual editing of outputs is still indispensable. In order to avoid this more research is required for developing methods which are fully automatic and accurate.

8.2 Building Detection, Extraction and Reconstruction

Airborne LiDAR data mostly contain information from the roofs of the buildings in the form of point cloud. Literature suggests that the roofs are assumed to be containing planar facets. Once the points belonging to a particular building are identified, detection of the individual planes is required. Some of the authors have also attempted to derive the

Table 1 Ground filtering algorithms

	Type of the algorithm	References
1	Morphological filters and their extension and variants	[41–44]
2	Active contouring	[45, 46]
3	Progressive densification	[40, 47–49]
4	Spline based method	[50, 51]
5	Surface based filters and their extension and variants	[52, 53]
6	Repetitive interpolation	[36]

building model parameters from the respective point cloud. The various approaches are summarized below and tabulated in Table 2:

Various techniques attempted for identification of planar surfaces in LiDAR data are as following:

1. *Hough transform* A plane can be represented either by its general equation, or by the triplet (ρ, θ, ϕ), which represents the direction of the normal to the plane. The Hough transform [65] identifies planes based on the orientation of most popular local normal through a voting process, which are identified by respective triplets. Plane identification for LiDAR data using the Hough transform has been studied by Overby et al. [54], Tasha-Kurdi et al. [55] and Lohani and Singh [66].
2. *RANSAC* Random Sample Consensus (RANSAC) is proposed by Fishler and Bolles [67], which chooses models based on a least squares regression, and has been used for the detection of planar facets by Forlani et al. [68], Tasha-Kurdi et al. [55], Nardinocchi et al. [56], Forlani et al. [69] and Bretar [57].
3. *Clustering of normals* Normals can be calculated by computing the Delaunay triangulation or the Voronoï diagram. Building facet detection by using clustering of normals has been used by Hofmann et al. [59], Morgan and Habib [60], Auer and Hinz [70] and Tse et al. [61].
4. *Octree and pseudo grid* The octree is a tree data structure, which divides the entire 3D space enveloping the point cloud. It is used for easier computational handling of a voluminous point cloud data. Plane detection using Octree data structure [71] has been done by Tseng and Wang [58]. On the other hand, Cho et al. [63] divided the areal extent of LiDAR dataset into a pseudo-grid and detected planes.
5. *Model description using invariant moments* Invariant moments [72] are used for visual pattern recognition specifically for shape analysis. Maas [73, 74] and Maas and Vosselman [64] have used first and second order invariant moments to derive building parameters.

Table 2 Plane extraction algorithms

	Type of the algorithm	References
1	Hough transform	[54, 55]
2	RANSAC	[56, 57]
3	Octree splitting and merging	[58]
4	Clustering of normals	[59–61]
5	Target based graph matching	[62]
6	Pseudo-grid based	[63]
7	Invariant moments	[64]

After the planar facets of the building roofs are identified, 3D models of the buildings are reconstructed. Bretar [57] comments that "the purpose of building reconstruction is to represent a building with as few point vertices as possible." In this process, the topological primitives and different connectivities are determined for the building. The various approaches for reconstructing the building models can be grouped as follows:

6. *Polyhedral models* Rottensteiner and Jansa [75] have used a raster-based approach, and they first group the detected segments using a 3–4 Chamfer mask as a proximity measure. This is followed by a boundary tracing and construction of walls and finally output as a wireframe model.
7. *Modelling using the ground plans* Brenner et al. [76] developed a heuristic subdivision of ground plans into rectangles as well as a rule-based reconstruction relying on discrete relaxation. Laycock and Day [77] have used the building footprint information to create the walls of the buildings. The roofs of the buildings have been modelled using a concept of "straight-skeletons". The fundamental units of modelling are rectilinear polygons and building models are derived by merging these fundamental units.
8. *Intersection of adjacent roof planes* Maas and Vosselman [64], Huber et al. [78], Forlani et al. [68], and Sampath and Shan [79] have used intersection of adjacent roof planes to create building model.
9. *Modelling using building primitives* Teo et al. [80] constructed building primitives and reconstructed the building using splitting and merging of these building primitives.

A summary of various approaches in the reconstruction of building models has been presented in Table 3.

Table 3 Reconstruction of building models

	Type of the algorithm	References
1	Hough transform	[54, 55, 81]
2	RANSAC	[57, 81]
3	Octree splitting and merging	[58]
4	Clustering of normals	[59]
5	Target based graph matching	[62]
6	Pseudo-grid based	[63]
7	Invariant moments	[73]
8	Intersection of planar faces	[74]
9	Polyhedral building roofs	[79, 82]

8.3 Tree Classification

An exhaustive review of forest related studies from LiDAR data has been presented in Hyyppä et al. [83]. Although the extraction of various tree or forest parameters from LiDAR data has been made possible by various researchers, not much has been said about the representation of trees on a visualization engine. Fujisaki et al. [84] have used a simple forest model to represent trees. Morsdorf et al. [85] have used clustering algorithms to detect trees and then use convex hulls to represent them. Another team extended their previous work, and used rotational paraboloids and cylinders to represent tree canopies and trunks, respectively [86].

Tree locations can be determined using point cloud local maxima [87]. Using canopy height model (CHM) and segmentation methods, Hyyppä and Inkinen [87] and, Friedlaender and Koch [88] have demonstrated individual-tree based forest inventory. DSM or CHM images have also been used for individual tree crown (ITC) or crown diameter estimation [89, 90]. Detection of trees and large scale visualization for urban landscapes have been attempted by Oehlke et al. [91]. LiDAR data have been shown useful in biomass estimation and carbon stock assessment.

8.4 Road Detection

Literature on identification of points belonging to roads can be classified into the following groups: (1) integration of imagery and LiDAR data, (2) integration of existing maps and LiDAR data, and (3) morphological filtering, (4) road extraction using graph theoretic concepts, (5) buffering method (6) classifier selection strategy, and (7) use of range, intensity and elevation images in classification. Literature found in the above groups are listed in Table 4.

Table 4 Summary of road detection algorithms

	Type of the algorithm	References
1	Integration of imagery and LiDAR data	[92–94]
2	Integration of existing maps and LiDAR data	[95, 96]
3	Morphological filtering using intensity and range data	[97]
4	Graph theoretic concepts	[98]
5	Buffering method	[99]
6	Classifier selection strategy	[100]
7	Range, intensity and elevation images with EM classification	[101]

In the given list of literature for road detection, Clode et al. [102] and Zhao et al. [101] have attempted the vectorisation of roads for making maps.

8.5 Segmentation Based Methods

The segmentation based methods for LiDAR data are found to be either raster based or point cloud based. The idea of segmentation is to partition a point cloud into different groups based on certain properties set by the algorithm. The conversion of LiDAR data into a raster, results in the loss of three-dimensional information. Also, segmentation on a raster can result in inaccuracies. On the other hand, segmentation on the point clouds are usually terrain feature focussed, i.e. ground, non-ground or building, non-building etc.

In the point cloud based methods, buildings were extracted by using scan line segmentation [103]. Shan and Sampath [104] developed a method to separate ground and non-ground points, and Chehata [105] used hierarchical k-means to separate ground, off-ground and low-off ground classes. However, Chehata's approach is not suitable for steep terrains. Separation of buildings and non-building points was done by Filin and Pfeifer [43] using a slope adaptive neighbourhood technique.

In the grid based methods, Samadzadegan et al. [106] used multi-class Support Vector Machines (SVMs) on grids derived from LiDAR data to extract different classes. Brattberg and Tolt [107] first separated ground and non-ground pixels and then used an object based classification to detect buildings.

8.6 Visual Analytics Based Approach

Visual analytics has potential to play significant role in improving structural classification and semantic classification of 3D LiDAR point clouds. Kumari et al. [108] have proposed an approach using Compute Unified Device Architecture (CUDA) [109],which includes outlier detection, geometric classification, feature detection, line feature

extraction, and down-sampling [110]. In order to alleviate the gap of unsupervised machine learning algorithms in semantic classification of LiDAR point clouds, the authors have proposed a visualization-driven technique for deciding clustering parameters for a hierarchical divisive classification [111]. They have implemented a prototype tree visualizer tool for hierarchical Expectation–Maximization technique, where the overall accuracy of around 70% [112] allowed for quick assessment of datasets. The tree visualizer tool developed allows user to consult the colormaps (or heatmaps) of different parameters used for semantic classification for determining the parameter that gives the best binary classification. Structural classes give information of the likelihood of a point belonging to a surface, line, or degenerate point (or junction) types of features in the region. The authors there by propose a tuple of structural and semantic classes, calling it an *augmented semantic classification* [111] for labeling the points, e.g. (line, building), (surface, building), etc. The authors have reported that augmented semantic classification gives better quality rendering of point clouds for visualization, especially where line feature points highlight boundaries or edges. Structural classification is derived from conventionally used covariance analysis, which gives the shape of the local neighborhood of each point [108, 110]. However, it was found that the local geometric descriptor, upon eigenvalue analysis, does not detect sharp line features, e.g. gabled roof lines, and unoriented points, e.g. foliage, accurately [111]. However, a tensor voting based local geometric descriptor improves the structural classification [112, 113]. The proposed local geometric descriptor detected line features in gabled roofs, however, detecting un-oriented points in foliage is not satisfactory. The authors have further proposed the use of gradients of two-dimensional local geometric descriptor for correcting the classification of such points as point-type features [114] and also used the Gradient Energy Tensor [115] to identify points of interest, i.e., the foliage points.

8.7 Convolutional Neural Networks Based LiDAR Data Classification

Deep convolutional neural networks (CNN) have gained lot of popularity in object recognition research from images. This is because of their higher classification accuracy compared to traditional methods and parameter independency. Recently researchers have started investigating the use of CNN for classification of point cloud data in general and LiDAR data in particular. Kumar et al. [116] have proposed a CNN architecture for automatic classification of LiDAR data obtained for outdoor environment. LiDAR data have noise, clutter, high point density and large size in comparison to images. The authors have developed an architecture which deals with the problem of geometry loss during rescaling of point cloud, given the constraint of fixed number of neurons in CNN and have also proposed a method to minimize the loss of data points due to voxelization. The authors have reported classification accuracies ranging from 85 to 92.5% with kappa values ranging from 75 to 83.5% in different cases of input data. This work is currently for mobile LiDAR data, however, the same approach can be easily extended for airborne data. As claimed by the authors, the reported accuracies may be improved further by employing better computing facilities and providing extended training to the CNN developed.

9 Future Scope of Technology, Related Research and Conclusion

LiDAR data have the ability to capture and represent our physical environment like never before. All physical phenomena that happen in our surrounding across wide range of scales highly depend on the physical landscape. LiDAR is being used in applications like flood modelling, sound propagation modelling [117], electromagnetic wave propagation modelling among others. There are still a large number of problem domains similar to the above where LiDAR would find use, e.g. air pollution propagation, sunlight availability analysis, air movement corridor analysis in urban environment etc.

The 3D Elevation Programme (3DEP) of the USGS for US is an important area where the LiDAR data are expected to play a major role. It is quite likely that similar programmes would be extended globally. Stoker et al. [13] have evaluated different sensors for this program. There is a need to develop such program for India where a lot of research has to be done to choose the right technology and specifications of such elevation dataset.

The use of LiDAR from Unmanned Aerial Vehicles (UAV) has already started. However, its commercial application is still negligible compared to its counterpart, i.e., photogrammetry based systems. With the sensors becoming smaller and data processing technologies like Simultaneous Localisation and Mapping (SLAM) becoming stronger, there will be much wider use of these UAV LiDARs in near future. Generation of large volumes of LiDAR data and in several cases time-series of data would require development of better processing techniques. Data captured by Geokno India Pvt. Ltd. in India for ravines amply demonstrate the possibility of use of these data for ravine reclamation, whereas other techniques fail to map ravines.

As has been seen in this paper, a variety of approaches have been used for data understanding through classification. However, a large part of data processing still hinges

on manual input. It is expected that artificial intelligence and deep learning techniques would find much more use in understanding LiDAR data. LiDAR data can be represented in a large number of feature classes based on geometric parameters-local and global. A large number of such features have been already studied. However, there is a need to collate all such features in a place (similar to eCognition Software approach for images) and develop classification techniques based on these.

This review paper has outlined the state-of-the-art LiDAR sensors and their relative advantages. The paper dwells upon the flight planning issue for an airborne platform and has emphasized the use of optimization based approach for minimizing the cost of project. The paper also discussed the accuracy and data quality issues of LiDAR data and the methods to quantify these. The paper has discussed conventional approaches for LiDAR data classification for different object classes, e.g., ground, building, tree, road etc. More importantly the paper has also highlighted the use of some recent approaches for data classification which are based on visual analytics and CNN. The paper has successfully brought all these diverse aspects associated with LiDAR technology in one place and also highlighted the important research issues where work would focus in future.

References

1. Ritchie JD (1996) Airborne laser altimeters, remote sensing applications to hydrology. Hydrol Sci J 41(4):625–636
2. Rempel RC, Parker AK (1964) An information note on an airborne laser terrain pprofile for micro-relief studies. In: Proceedings of the 3rd symposium on remote sensing of environment, University of Michigan Institute of Science and Technology
3. Hickman GD, Hogg JE (1969) Application of an airborne pulsed laser for near shore bathymetric measurements. Remote Sens Environ 1:47–58
4. Hoge FE (1988) Airborne oceanographic LiDAR (AOL) flight mission participation. In: Laboratory for oceans. National Aeronautics and Space Administration, Goddard Space Flight Center, Greenbelt, pp 95–97
5. Krabill WB, Collins JG, Link LE, Swift RN, Butler ML (1984) Airborne laser topographic mapping results. Photogramm Eng Remote Sens 50:685–694
6. Schreier H, Lougheed J, Tucker C, Leckie D (1983) Automated measurements of terrain reflection and height variations using and Airborne infrared laser system. Int J Remote Sens 6(1):101–113
7. Hoge FE (1974) Integrated laser/radar satellite ranging and tracking system. Appl Opt 13(10):2352–2358
8. Arp H, Griesba JC, Burns JP (1982) Mapping in tropical forests: a new approach using the laser APR. Photogramm Eng Remote Sens 48(1):91–100
9. Hofton MA et al (2000) An airborne laser altimetry survey of Long Valley California. Int J Remote Sens 21(12):2413–2437
10. Wagner W, Ullrich A, Ducic V, Melzer T, Studnicka N (2006) Gaussian decomposition and calibration of a novel small-footprint full-waveform digitizing airborne laser scanner. ISPRS J Photogramm Remote Sens 60(2):100–112
11. Doneus M, Briese C, Fera M, Janner M (2008) Archaeological prospection of forested areas using full-waveform airborne laser scanning. J Archaeol Sci 35(4):882–893
12. Xiaoliang Z, Guihua Z, Jonathan L, Yuanxi Y, Yong F (2016) 3D land cover classification based on multispectral LiDAR point clouds. Int Arch Photogramm Remote Sens Spat Inf Sci 41(B1):741–747
13. Stoker JM, Abdullah QA, Nayegandhi A, Winehouse J (2016) Evaluation of single photon and geiger mode lidar for the 3D elevation program. Remote Sens 8(9):767
14. Dashora A (2013) Optimization system for flight planning for airborne LiDAR data aquisition. Indian Institute of Technology Kanpur, Kanpur
15. Dashora A, Lohani B (2013) LiDAR technology and a new method of flight planning for airborne LiDAR data acquisition. In: ISRS–ISG conference, Vishakhapattanam
16. Dashora A, Lohani B, Deb K (2014) Method of flight planning for airborne LiDAR using genetic algorithms. SPIE J Appl Remote Sens 8(1):1–19
17. Dashora A, Lohani B, Deb K (2014) LiDAR flight planning—a new system for flight planning with minimal user intervention. GIM Int Mag. https://www.gim-international.com/content/article/lidar-flight-planning
18. Dashora A, Lohani B, Deb K (2013) Turning mechanisms for airborne LiDAR and photographic data acquisition. SPIE J Appl Remote Sens 7(1):1–19
19. Dashora A, Lohani B, Deb K (2013) Two-step procedure of optimization for solving the flight planning problem for airborne LiDAR data acquisition. Int J Math Model Numer Optim 4(4):323–350
20. Dashora A, Lohani B, Deb K (2012) Flight planning system for airborne data acquisition
21. ASPRS (2011) ASPRS LAS format standard 1.4
22. Heidemann HK (2014) Lidar base specification (ver. 1.2, November 2014) (USGS)
23. Casella V, Spalla A (2000) Estimation of horizontal accuracy of laser scanning data. Proposal of a method exploiting ramps. Int Arch Photogramm Remote Sens 33(B3):157–163
24. Vosselman G (2008) Analysis of planimetric accuracy of airborne laser scanning surveys. Int Arch Photogramm Remote Sens Spat Inf Sci XXXVII(B3a):99–104
25. Kreylos O, Bawden GW, Kellogg LH (2008) Immersive visualization and analysis of LiDAR data. In: Bebis G et al (eds) Advances in visual computing. ISVC 2008. Lecture notes in computer science, vol 5358. Springer, Berlin, Heidelberg
26. Richter R, Döllner J (2010) Out-of-core real-time visualization of massive 3D point clouds. In: Proceedings of the 7th international conference on computer graphics, virtual reality, visualisation and interaction in Africa. ACM, Franschhoek, pp 121–128
27. Stoker JM (2004) Voxels as a representation of multiple-return lidar data. In: Proceedings of ASPRS annual conference, Denver
28. Stoker JM (2009) Volumetric visualization of multiple-return LIDAR data: using voxels. Photogramm Eng Remote Sens 75(2):109–112
29. Isenburg M, Liu Y, Shewchuk J, Snoeyink J, Thirion T (2006) Generating raster DEM from mass points via TIN streaming. In Proceedings of the 4th international conference on geographic information science
30. Ghosh S, Lohani B (2015) Development and comparison of aerial photograph aided visualization pipelines for LiDAR datasets. Int J Digital Earth 8(8):656–677

31. Ghosh S, Lohani B (2013) Mining LiDAR data with spatial clustering algorithms. Int J Remote Sens 34(14):5119–5135
32. Ester M, Kriegel H-P, Sander Jo, Xu X (1996) A density-based algorithm for discovering clusters in large spatial databases with noise. In: Proceedings of the second international conference on knowledge discovery and data mining (KDD-96). AAAI Press, pp 226–231
33. Ankrest M, Breunig M, Kriegel HP, Sander J (1999) OPTICS: ordering points to identify the clustering structure. In Proceedings of ACM, SIGMOD'99
34. Ghosh S, Lohani B, Misra N (2014) A study-based ranking of LiDAR data visualization schemes aided by georectified aerial images. Cartogr Geogr Inf Sci 41(2):138–150
35. Sithole G, Vosselman G (2004) Experimental comparison of filter algorithms for bare-earth extraction from airborne laser scanning point clouds. ISPRS J Photogramm Remote Sens 59:85–101
36. Kobler A et al (2007) Repetitive interpolation: a robust algorithm for DTM generation from Aerial laser scanner data in forested terrain. Remote Sens Environ 108:9–23
37. Pfeifer N, Mandlburger G (2008) LiDAR data filtering and DTM generation. In: Topographic laser ranging and scanning: principles and processing, pp 308–333
38. Meng X, Currit N, Zhao K (2010) Ground filtering algorithms for airborne LiDAR data: a review of critical issues. Remote Sens 2(3):833–860
39. Sithole G, Vosselman G (2003) Automatic structure detection in a point-cloud of an urban landscape. In 2nd GRSS/ISPRS joint workshop on remote sensing and data fusion over urban areas, pp 67–71
40. Błaszczak-Bąk W, Janowski A, Kamiński W, Rapinski J (2011) Optimization algorithm and filtration using the adaptive TIN model at the stage of initial processing of the ALS point cloud. Can J Remote Sens 37(6):583–589
41. Roggero M (2001) Airborne laser scanning: clustering in raw data. Int Arch Photogramm Remote Sens 3/W4 34:227–232
42. Sithole G (2001) Filtering of laser altimetry data using a slope adaptive filter. Int Arch Photogramm Remote Sens Spat Inf Sci XXXIV(3/4):203–210
43. Filin S, Pfeifer N (2006) Segmentation of airborne laser scanning data using a slope adaptive neighbourhood. ISPRS J Photogramm Remote Sens 60:71–80
44. Meng X, Wang L, Silván-Cárdenas JL, Currit N (2009) A multi-directional ground filtering algorithm for airborne LIDAR. ISPRS J Photogramm Remote Sens 64(1):117–124
45. Elmqvist M (2002) Ground surface estimation from airborne laser scanner data using active shape models. In: Photogrammetric computer vision, ISPRS commission III symposium, Graz
46. Elmqvist M (2001) Ground estimation of laser radar data using active shape models. In: OOPE workshop on airborne laser scanning and interferometric SAR for detailed digital elevation models
47. Axelsson P (2000) DEM Generation from laser scanner data using adaptive TIN models. In IAPRS, XXXIII, B4/1, Amsterdam
48. Axelsson P (1999) Processing of laser scanner data—algorithms and applications. ISPRS J Photogramm Remote Sens 54(2–3):138–147
49. Sohn G, Dowman I (2002) Terrain surface reconstruction by the use of tetrahedron model with the MDL Criterion. Int Arch Photogramm Remote Sens Spat Inf Sci XXXIV(Pt. 3A):336–344
50. Brovelli MA, Cannata M, Longoni UM (2004) LIDAR data filtering and DTM interpolation within GRASS. Trans GIS 8(2):155–174
51. Brovelli MA, Cannata M, Longoni UM (2002) Managing and processing LIDAR data within GRASS. In: Proceedings of GRASS users conference, Trento, Italy, 11–13 Sept, p 29
52. Kraus K, Pfeifer N (1997) A new method for surface reconstruction from laser scanner data. In: IAPRS, XXXII, 3/2W3, Haifa, Israel
53. Lohmann P, Koch A, Schäffer M (2000) Approaches to the filtering of laser scanner data. Int Arch Photogramm Remote Sens XXXIII(B3/1):534–541
54. Overby J, Bodum L, Kjems E, Iisoe PM (2004) Automatic 3D building reconstruction from airborne laser scanning and cadastral data using Hough transform. Int Arch Photogramm Remote Sens XXXV(B3):296–301
55. Tarsha-Kurdi F, Landes T, Grussenmeyer P (2007) Hough-transform and extended RANSAC Algorithms for automatic detection of 3D building roof planes from LiDAR data. In: International Archives of Photogrammetry and Remote Sensing, Espoo
56. Nardinocchi C, Scaioni M, Forlani G (2001) Building extraction from LIDAR data. In: Remote sensing and data fusion over urban areas, IEEE/ISPRS joint workshop 2001, pp 79–84
57. Bretar F (2008) Feature extraction from LiDAR data in urban areas. In: Topographic laser ranging and scanning: principles and processing, pp 403–419
58. Tseng Y-H, Wang M (2005) Automatic plane extraction from LIDAR data based on octree splitting and merging segmentation. In Geoscience and remote sensing symposium, 2005. IGARSS '05. Proceedings. 2005 IEEE International, pp 3281–3284
59. Hofmann AD, Maas H-G, Streilein A (2003) Derivation of roof types by cluster analysis in parameter spaces of airborne laser-scanner point clouds. In ISPRS commission III WG3, workshop, 3-D reconstruction from airborne laserscanner and InSAR data, IAPRS international archives of photogrammetry and remote sensing and spatial information sciences, vol 34, part 3/W13, pp 112–117
60. Morgan M, Habib A (2002) Interpolation of LiDAR data and automatic building extraction. In: ACSM-ASPRS 2002 annual conference proceedings
61. Tse R, Gold C, Kidner D (2007) Using the delaunay triangulation/voronoi diagram to extract building information from raw LIDAR data. In 4th International symposium on voronoi diagrams in science and engineering, 2007. ISVD '07, pp 222–229
62. Oude Elberink S, Vosselman G (2009) Building reconstruction by target based graph matching on incomplete laser data: analysis and limitations. Sensors 9(8):6101–6118
63. Cho W, Jwa Y-S, Chang H-J, Lee S-H (2004) Pseudo-grid based building extraction using airborne LIDAR data. In International archives of photogrammetry and remote sensing, pp 378–381
64. Maas HG, Vosselman G (1999) Two algorithms for extracting building models from raw laser altimetry data. ISPRS J Photogramm Remote Sens 54:153–163
65. Hough PVC (1962) Methods and means for recognizing complex patterns
66. Lohani B, Singh R (2008) Effect of data density, scan angle, and flying height on the accuracy of building extraction using LiDAR data. Geocarto Int 23(2):81–94
67. Fischler MA, Bolles RC (1981) Random sample consensus: a paradigm for model fitting with applications to image analysis and automated cartography. Commun ACM 24(6):381–395
68. Forlani G, Nardinocchi C, Scaioni M, Zingaretti P (2006) Complete classification of raw LIDAR data and 3D reconstruction of buildings. Pattern Anal Appl 8:357–374
69. Forlani G, Nardinocchi C, Scaioni M, Zingaretti P (2003) Building reconstruction and visualization from LiDAR data. In: The international archives of the photogrammetry, remote sensing and spatial information sciences, Ancona

70. Auer S, Hinz S (2007) Automatic extraction of salient geometric entities from LIDAR point clouds. In Geoscience and remote sensing symposium, 2007. IGARSS 2007. IEEE International, pp 2507–2510
71. Donald M (1980) Octree encoding: a new technique for the representation, manipulation and display of arbitrary 3-D objects by computer. Rensselaer Polytecnic Institute, Troy
72. Ming-Kuei H (1962) Visual pattern recognition by moment invariants. IEEE Trans Inf Theory 8(2):179–187
73. Maas H-G (1999) Closed solutions for the determination of parametric building models from invariant moments of airborne laserscanner data. In ISPRS conference 'Automatic extraction of GIS objects from digital imagery', Munich, September 6–10, pp 193–199
74. Maas HG (1999) Fast determination of parametric house models from dense airborne laserscanner data. Int Arch Photogramm Remote Sens XXXII(2W1):1–6
75. Rottensteiner F, Jansa J (2002) Automatic extraction of buildings from lidar data and aerial images. In ISPRS commission IV, symposium, Ottawa
76. Brenner C, Haala N, Fritsch D (2001) Towards fully automated 3D city model generation. In: Ascona01, pp 47–57
77. Laycock RG, Day AM (2003) Rapid generation of urban models. Comput Gr 27(3):423–433
78. Huber M, Schickler W, Hinz S, Baumgartner A (2003) Fusion of LiDAR data and aerial imagery for automatic reconstruction of building surfaces. In: 2nd GRSS/ISPRS workshop on "Data fusion and remote sensing over urban areas", pp 82–86
79. Sampath A, Shan J (2010) Segmentation and reconstruction of polyhedral building roofs from aerial lidar point clouds. IEEE Trans Geosci Remote Sens 48(3):1554–1567
80. Teo TA, Rau JY, Chen LC, Liu JK, Hsu WC (2006) Reconstruction of complex buildings using LIDAR and 2D maps. In: Abdul-Rahman A, Zlatanova S, Coors V (eds) Innovations in 3D geo information systems. Lecture notes in geoinformation and cartography. Springer, Berlin, Heidelberg
81. Zaharia T, Prêteux F (2002) Shape based retrieval of 3D mesh models. In: Proceedings of the IEEE international conference on multimedia and expo, 2002. ICME'02, pp 437–440
82. Chen L-C, Teo T-A, Kuo C-Y, Rau J-Y (2008) Shaping polyhedral buildings by the fusion of vector maps and lidar point clouds. Photogramm Eng Remote Sens 74(9):1147–1157
83. Hyyppä J et al. (2008) Forest inventory using small-footprint airborne LiDAR. In: Topographic laser ranging and scanning: principles and processing, pp 335–370
84. Fujisaki I et al (2008) Stand assessment through LiDAR-based forest visualization using a stereoscopic display. For Sci 54(1):1–7
85. Morsdorf F, Meier E, Allgöwer B, Nüesch D (2003) Clustering in airborne laser scanning raw data for segmentation of single trees. In: International archives of the photogrammetry, remote sensing and spatial information sciences
86. Morsdorf F et al (2004) LIDAR-based geometric reconstruction of boreal type forest stands at single tree level for forest and wildland fire management. Remote Sens Environ 92:353–362
87. Hyyppä J, Inkinen M (1999) Detecting and estimating attributes for single trees using laser scanner. Photogramm J Finl 16:27–42
88. Friedlaender H, Koch B (2006) First experience in the application of laser scanner data for the assessment of vertical and horizontal forest structures. In: International archives of photogrammetry and remote sensing, vol XXXIII, B7. ISPRS Congress, Amsterdam
89. Brandtberg T, Warner T, Landenberger R, McGraw J (2003) Detection and analysis of individual tree crowns in small footprint, high sampling density LiDAR data from the eastern deciduous forest in North America. Remote Sens Environ 85:290–303
90. Tiede D, Hoffman C (2006) Process oriented object-based algorithms for single tree detection using laser scanning. In International workshop 3D remote sensing in forestry proceedings, Vienna, 14–15 Feb 2006
91. Oehlke C, Richter R, Döllner J (2015) Automatic detection and large-scale visualization of trees for digital landscapes and city models based on 3D point clouds. In: 16th Conference on digital landscape architecture (DLA 2015), pp 151–160
92. Shamayleh H, Khattak A (2003) Utilization of LiDAR technology for highway inventory. In Proceedings of the 2003 midcontinent transportation research symposium, Ames
93. Harvey WA, McKeown Jr. DM (2008) Automatic compilation of 3D road features using LIDAR and multi-spectral source data. In: ASPRS 2008
94. Tiwari P, Pande H, Pandey A (2009) Automatic urban road extraction using airborne laser scanning/altimetry and high resolution satellite data. J Indian Soc Remote Sens 37:223–231
95. Vosselman G (2003) 3D reconstruction of roads and trees for city modelling. In: 3-D reconstruction from airborne laserscanner and InSAR data, Dresden
96. Oude Elberink S, Vosselman G (2006) 3D modelling of topographic objects by fusing 2D maps and lidar data. Int Arch Photogramm Remote Sens Spat Inf Sci XXXVI(4):27–30
97. Clode S, Rottensteiner F, Kootsookos PJ (2005) Improving city model determination by using road detection from LiDAR data. In: Joint workshop of ISPRS and the German Association for Pattern Recognition (DAGM), 'Object extraction for 3D city models, road databases and traffic monitoring—concepts, algorithms, and evaluation' (CMRT05), Vienna
98. Zhu P, Lu Z, Chen X, Honda K, Eiumnoh A (2004) Extraction of city roads through shadow path reconstruction using laser data. Photogrammetric Engineering and Remote Sensing 70(12):1433–1440
99. Choi Y-W, Jang Y-W, Lee H-J, Cho G-S (2008) Three-dimensional LiDAR data classifying to extract road point in urban area. IEEE Geosci Remote Sens Lett 5(4):725–729
100. Samadzadegan F, Hahn M, Bigdeli B (2009) Automatic road extraction from LIDAR data based on classifier fusion. In: Urban remote sensing event, 2009 joint, pp 1–6
101. Zhao J, You S, Huang J (2011) Rapid extraction and updating of road network from airborne LiDAR data. In: Applied imagery pattern recognition workshop (AIPR). IEEE, pp 1–7
102. Clode S, Rottensteiner F (2005) Classification of trees and powerlines from medium resolution airborne laserscanner data in urban environments. In: *WDIC*, pp 191–196
103. Sithole G, Vosselman G (2005) Filtering of airborne laser scanner data based on segmented point clouds. Int Arch Photogramm Remote Sens Spat Inf Sci XXXVI(3/W19):66–71
104. Shan J, Sampath A (2005) Urban DEM generation from raw lidar data: a labelling algorithm and its performance. Photogramm Eng Remote Sens 71(2):217–226
105. Chehata N, David N, Bretar F (2008) LIDAR Data Classification using Hierarchical k-means clustering. In: International archives of photogrammetry, remote sensing and spatial information sciences. Beijing, pp 325–330
106. Samadzadegan F, Bigdeli B, Ramzi P (2010) A multiple classifier system for classification of LIDAR remote sensing data using multi-class SVM. In: El Gayar N, Kittler J, Roli F (eds) Multiple classifier systems. MCS 2010. Lecture notes in computer science, vol 5997. Springer, Berlin, Heidelberg
107. Brattberg O, Tolt G (2008) Terrain classification using airborne lidar data and aerial imagery. In: The international archives of the photogrammetry, remote sensing and spatial information sciences. Beijing, pp 261–266
108. Kumari B, Ashe A, Sreevalsan Nair J (2014) Remote interactive visualization of parallel implementation of structural feature

extraction of three-dimensional lidar point cloud. In: Third international conference big data analytics, BDA 2014. New Delhi, India, 2–23 December 2014. Springer, pp 129–132
109. NVIDIA (2008) NVIDIA CUDA programming guide 2.0, NVIDIA Corporation
110. Keller P et al (2011) Extracting and visualizing structural features in environmental point cloud LiDaR data sets. In: Topological methods in data analysis and visualization: theory, algorithms, and applications, Springer, pp 179–192
111. Kumari B, Sreevalsan-Nair J (2015) An interactive visual analytic tool for semantic classification of 3D urban LiDAR point cloud. In: Proceedings of the 23rd SIGSPATIAL international conference on advances in geographic information systems, ACM, Seattle, pp 71–73
112. Kumari B (2016) Visualization techniques in classification of 3D urban LiDAR point cloud. Master of Science by Research, IIIT Bangalore
113. Sreevalsan Nair J, Kumari B (2017) Local geometric descriptors for multi-scale probabilistic point classification of airborne LiDAR point clouds. Mathematics and Visualization 1–26 **(preprint)**
114. Sreevalsan-Nair J, Jindal A (2017) Using gradients and tensor voting in 3D local geometric descriptors for feature detection in airborne LiDAR point clouds in urban regions. In: Proceedings of 2017 IEEE international geoscience and remote sensing symposium, 2017 **(to appear)**
115. Felsberg M, Köthe U (2005) GET: the connection between monogenic scale-space and Gaussian derivatives. In: Scale space and PDE methods in computer vision, Springer, Berlin, pp 192–203
116. Kumar B, Lohani B, Pandey G (2017) Development of deep learning architecture for automatic classification of mobile LiDAR data. Int J Phtogramm Remote Sens **(communicated)**
117. Biswas S, Lohani B (2008) Development of high resolution 3D sound propagation model using LiDAR data and aerial photo. In: The international archives of the photogrammetry, remote sensing and spatial information sciences, Beijing